Journal of Ceramic Processing Research. Vol. 21, No. 3, pp. 296~301 (2020)
(Received 26 August 2019, Received in revised form 28 January 2020, Accepted 24 February 2020)
https://doi.org/10.36410/jcpr.2020.21.3.296

J O U R N A L O F
Ceramic Processing Research

Steam methane reforming performance of Ni/Al_2O_3 composite catalysts prepared *via* a hydrothermal-infiltration method

Sang-Hun Lee[a] and Ki-Tae Lee[b,c,*]
[a]*Coseal Co. LTD., Jeonbuk, 54008 Republic of Korea*
[b]*Division of Advanced Materials Engineering, Jeonbuk National University, Jeonbuk, 54896 Republic of Korea*
[c]*Hydrogen and Fuel Cell Research Center, Jeonbuk National University, Jeonbuk, 54896 Republic of Korea*

Ni as a catalyst for steam methane reforming (SMR) was deposited on a porous Al_2O_3 support using a hydrothermal-infiltration method. The SMR performance of Ni/Al_2O_3 composites was strongly affected by the microstructural change of the support according to the firing temperature. While there was no significant change up to 800 °C, significant grain growth and large interfacial necking occurred after firing at 1,200 °C, resulting in a significant increase in both porosity and pore size. The Al_2O_3 support with a large pore size and broad pore size distribution could load a relatively larger amount of Ni catalyst during the hydrothermal-infiltration process and facilitate the diffusion of reaction gases. Therefore, the Ni/Al_2O_3 composite with the support fired at 1,200 °C exhibited the best SMR performance. Meanwhile, Ni catalysts were distributed evenly throughout the porous support in the Ni/Al_2O_3 composite prepared by the hydrothermal-infiltration method compared to that prepared by the conventional infiltration method. Therefore, the Ni/Al_2O_3 composite prepared by the hydrothermal-infiltration method exhibited much better SMR performance. Moreover, no significant performance degradation was observed at 600 °C for 100 h.

Keywords: Hydrogen production, Steam methane reforming, Catalyst, Hydrothermal-infiltration method.

Introduction

Hydrogen has attracted much attention as an alternative energy source due to its high energy density, abundance, and eco-friendliness [1-4]. Among many hydrogen production methods, the steam methane reforming (SMR) method *via* the reaction of methane and water is well known to be cost-effective [5-7]. The SMR reaction can be described as follows:

$$CH_4\ (g) + H_2O\ (g) = 3H_2\ (g) + CO\ (g) \quad (1)$$

$$CO\ (g) + H_2O\ (g) = H_2\ (g) + CO_2\ (g) \quad (2)$$

While the first reaction is strongly endothermic, the second reaction, called the water-gas shift reaction, is slightly exothermic [8,9]. In general, metal based-catalysts such as Ni, Co, Ru, Rh, Pd, and Pt are used to improve the performance of the SMR process [10-16]. While noble metal-based catalysts are expensive and have limitations in mass production and industrialization, Ni has been widely used due to its low cost and high catalyst performance [17-20].

A Ni catalyst for SMR is generally used in the form of a composite coated on a porous support such as Al_2O_3. Therefore, it is an important issue to distribute the Ni catalyst evenly over the support. The infiltration method is the most widely used because the solution-based process is very simple and does not need high temperature sintering accompanied by grain growth of the catalyst [21-23]. When the porous support is immersed in the precursor solution of the catalyst in the infiltration method, the precursor solution penetrates into the pores of the support by capillary forces. Therefore, the deposition amount and distribution of the catalyst strongly depend on the microstructure of the support.

Meanwhile, the hydrothermal method is a well-known technique for the synthesis of high quality nano-powders. The hydrothermal method is also a solution-based process using an aqueous solution under high temperature at high vapor pressure [24-28]. One of the major advantages of the hydrothermal method is that nano-powders, which are not stable at elevated temperatures, can be synthesized. Nano-powders with high vapor pressures can also be produced by the hydrothermal method with minimum loss of materials. The compositions of nano-powders to be synthesized can be well-controlled through liquid phase or multiphase chemical reactions.

While the conventional infiltration method is limited by the capillary forces of the pores, the hydrothermal method might be less restrictive because of the high pressure. In this regard, herein we propose the hydrothermal-

*Corresponding author:
Tel : +82-63-270-2290
Fax: +82-63-270-2386
E-mail: ktlee71@jbnu.ac.kr

infiltration method, which can distribute the catalyst evenly throughout the porous support by the driving force of high temperature and high pressure. In this study, Ni as a catalyst was deposited on an Al_2O_3 support using the hydrothermal-infiltration method. The microstructure and SMR performance of Ni/Al_2O_3 composite catalysts synthesized by the hydrothermal-infiltration method were compared with those of the catalyst prepared by the conventional infiltration method and commercial SMR catalysts.

Experimental Procedure

Ni/Al_2O_3 composite catalysts were prepared using the conventional infiltration method and the hydrothermal-infiltration method. $Ni(NO_3)_2 \cdot 6H_2O$ (> 99.0%, Sigma Aldrich, USA) was used for the precursor solution. De-ionized water was used for the aqueous phase. Porous Al_2O_3 (Puresorb, PA-AS2, Puresphere, Korea) was used as a support. To investigate the microstructural effect, Al_2O_3 supports were sintered at 500 °C, 800 °C, and 1,200 °C. Stock solutions containing 3 M Ni were prepared by dissolving the stoichiometric amount of $Ni(NO_3)_2 \cdot 6H_2O$ in de-ionized water. In the case of the infiltration method, an Al_2O_3 support was immersed in the Ni-precursor solution for 1 h at room temperature, followed by holding in a vacuum oven at 80 °C for 30 min. In the case of the hydrothermal-infiltration method, an Al_2O_3 support was also immersed in the Ni-precursor solution for 1 h at room temperature and then put into a hydrothermal autoclave reactor holding at 150 °C for 15 h. The Ni-impregnated Al_2O_3 supports were dried at 100 °C for 24 h and fired at 500 °C in air to remove organic substances and impurities, followed by final treatment at 800 °C in a 5% H_2/Ar atmosphere to obtain Ni/Al_2O_3 composites.

The phases of the as-synthesized Ni/Al_2O_3 composites were characterized by X-ray diffraction analysis (XRD; MAX-2500, Rigaku, Japan) using Cu (Kα) radiation. The morphology and microstructural characterizations were analyzed using high-resolution scanning electron microscopy/energy-dispersive X-ray spectroscopy (HR-SEM/EDX; SN-3000 Hitachi, Japan). The pore size and distribution were analyzed via mercury porosimetry analysis (Autopore IV, Micrometrics, USA), and the SMR performance was analyzed via gas chromatography (GC; YL6100GC, Youngin, Korea) from 300 °C to 800 °C. 10 g of Ni/Al_2O_3 and CH_4 with 20% H_2O was used as the catalyst and reforming gas, respectively. Long-term testing was also performed at 600 °C for 100 h to evaluate durability and performance retention. Meanwhile, a commercial Ni-based catalyst (HyProGen® R-70, Clariant) was used for the SMR performance comparison.

Results and Discussion

Microstructural changes of the Al_2O_3 support according to firing temperature are shown in Fig. 1. The as-received Al_2O_3 support had well-connected grains with a size of 50 nm. While there was no significant change in the microstructure after heat treatment up to 800 °C, significant grain growth and large interfacial necking

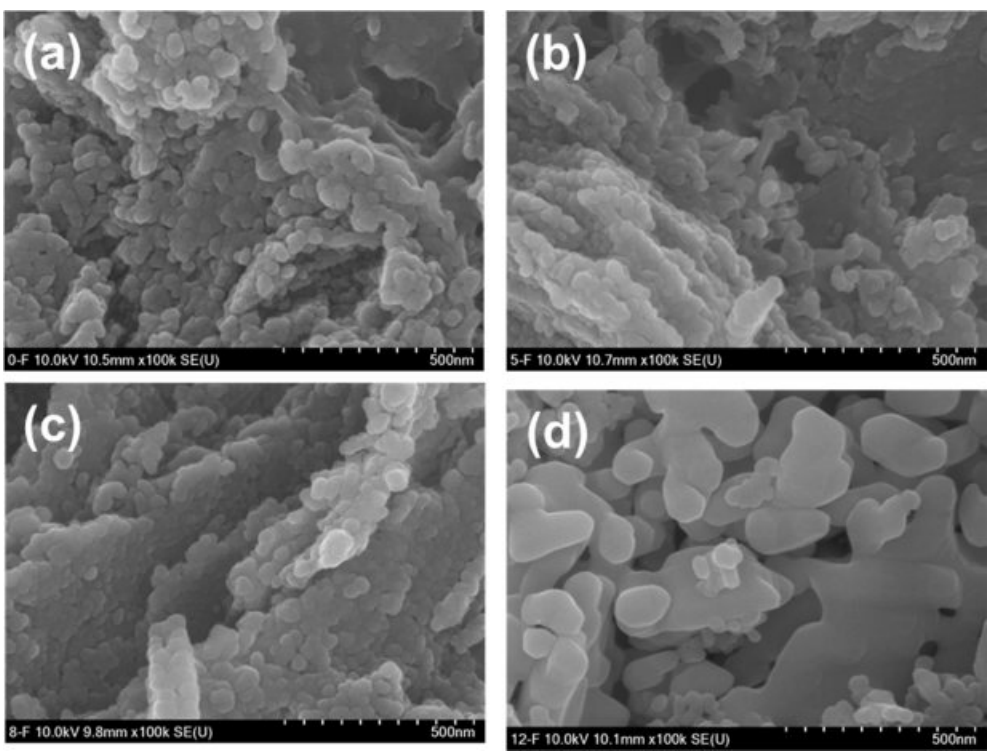

Fig. 1. HR-SEM images of (a) the as-received Al_2O_3 support and that fired at (b) 500 °C, (c) 800 °C, and (d) 1,200 °C.

occurred after firing at 1,200 °C. Fig. 2 shows the pore size distribution of the Al_2O_3 support according to the heat treatment, measured by the mercury porosimeter. The calculated porosity and median pore diameter based on the mercury porosimetry analysis are listed in Table 1. The as-received Al_2O_3 showed a porosity of 56.9% and a median pore diameter of 5.9 nm with a narrow pore size distribution. Both the porosity and median pore diameter increased gradually while retaining the narrow pore size distribution as the heat-treatment temperature increased up to 800 °C. On the contrary, dramatic changes in median pore diameter and pore size distribution were observed after firing at 1,200 °C. While there is no significant change in porosity, the median pore diameter of the support fired at 1,200 °C was 20 times larger than that of the as-received Al_2O_3 support. The pore size distribution also become very broad after firing at 1,200 °C. This behavior is due to significant grain growth and large interfacial necking at 1,200 °C, as shown in Fig. 1.

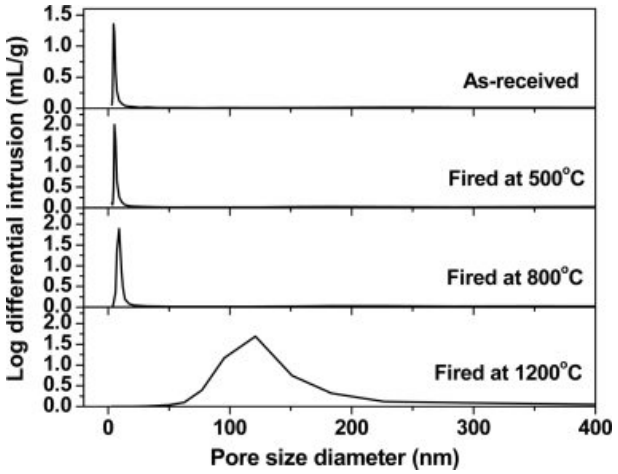

Fig. 2. Pore size distribution of the Al_2O_3 support according to heat-treatment temperatures.

The surface morphologies of the Ni/Al_2O_3 composites prepared by the hydrothermal-infiltration method according to the firing temperatures of the Al_2O_3 support are shown in Fig. 3. The fine Ni particles shown in bright colors

Table 1. Porosity and median pore diameter of the Al_2O_3 support according to the firing temperature, measured by a mercury porosimeter.

Firing temperature (°C)	Porosity (%)	Median pore diameter (nm)
As-received	56.9	5.6
500	58.9	6.4
800	60.5	9.6
1,200	65.3	131.1

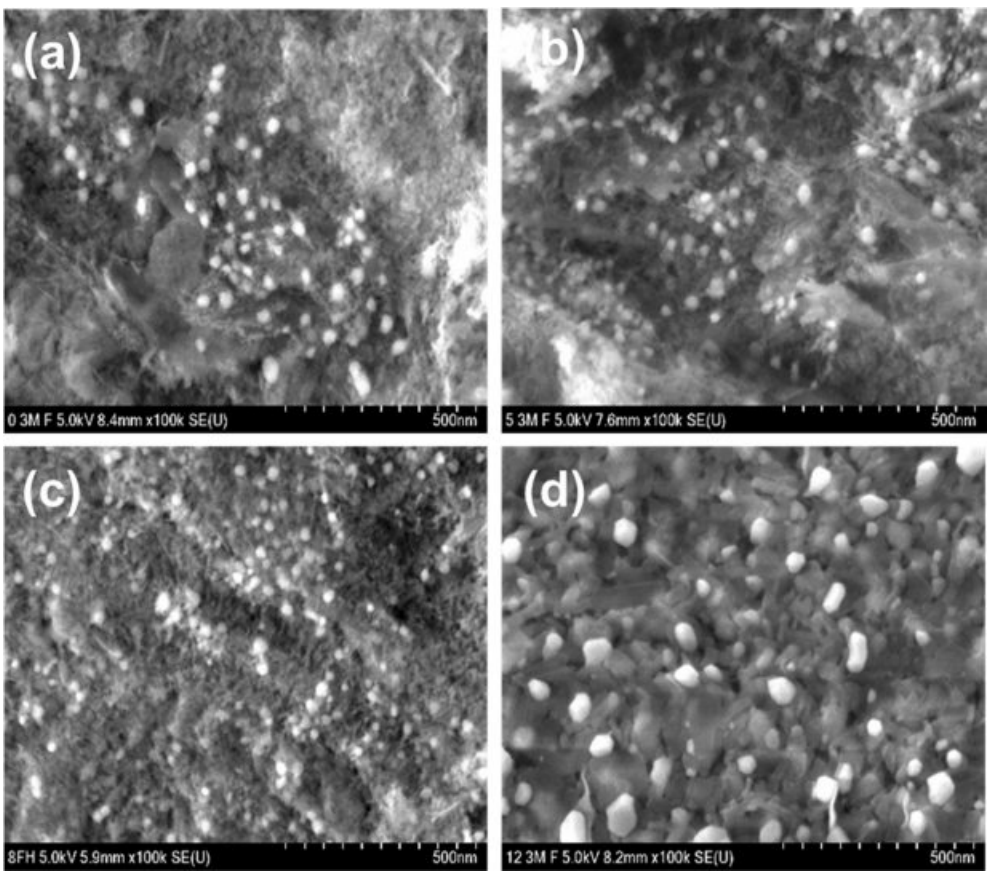

Fig. 3. HR-SEM images of the Ni/Al_2O_3 composites prepared by the hydrothermal-infiltration method with (a) a non-heat-treated, (b) 500 °C heat-treated, (c) 800 °C heat-treated, and (d) 1,200 °C heat-treated Al_2O_3 support.

in Fig. 3 were dispersed evenly on the Al_2O_3 support. In the case of the samples with the similar pore diameters as shown in Fig. 3(a)-(c), the grain sizes of Ni particles were similar. On the contrary, both the amount and grain size of the Ni particles increased in the case of the 1,200 °C heat-treated Al_2O_3 support (Fig. 3(d)). Basically, both the amount and size of the particles in the infiltration technique strongly depend on the porosity and pore size of the support because the amount of precursor solution infiltrated into the porous support is restricted by the pore channel. A relatively large amount of solution was infiltrated into the Al_2O_3 support fired at 1,200 °C where large pores existed, as shown in Fig. 1 and Table 1. The nucleation and grain growth might increase, resulting in the formation of Ni particles with relatively large sizes.

The SMR performance of the Ni/Al_2O_3 composite prepared by the hydrothermal-infiltration method with the Al_2O_3 support fired at various temperatures is shown in Fig. 4. The SMR performance improved as the firing temperature of the Al_2O_3 support increased. The 1,200 °C heat-treated Al_2O_3 support had relatively large pore sizes and a wide pore size distribution, as shown in Table 1 and Fig. 2. Therefore, a relatively large amount of Ni catalyst might be loaded into the support, and diffusion of the reaction gas is facilitated, resulting in the improved SMR performance.

Fig. 5 shows a comparison of the SMR performance of the Ni/Al_2O_3 composite according to the preparation technique. The Ni/Al_2O_3 composite prepared by the hydrothermal-infiltration method showed a much higher methane conversion ratio at the same reaction temperatures than that prepared by the conventional infiltration method. Moreover, the Ni/Al_2O_3 composite prepared by the hydrothermal-infiltration method exhibited better SMR performance than the commercial SMR catalyst.

XRD patterns of the Ni/Al_2O_3 composite according to the preparation technique are shown in Fig. 6. No secondary phases except Ni and Al_2O_3 were observed in any of the samples. This indicates that there is no change in phase or composition that affects SMR performance according to the preparation technique. In other words, the difference in the SRM performance between the samples prepared by the conventional infiltration method and the samples prepared by the hydrothermal-infiltration method is mainly due to the microstructure rather than a change in phase or composition.

EDX analysis for the fractured Ni/Al_2O_3 composite was carried out to verify the amount of Ni catalysts from surface to interior, and the elemental analysis data are listed in Table 2. The Ni content on the surface and inside the composite prepared by the hydrothermal-infiltration method was similar. On the contrary, there were much more Ni catalyst on the surface than inside the composite prepared by the conventional infiltration method. A schematic illustration of the Ni/Al_2O_3

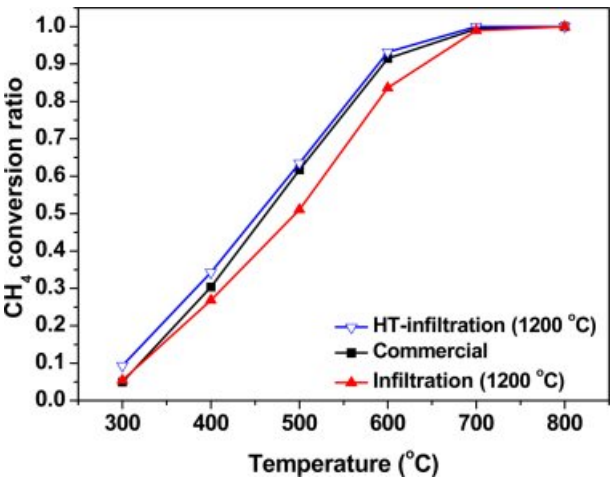

Fig. 5. Comparison of the SMR performance of the Ni/Al_2O_3 composite according to the preparation technique.

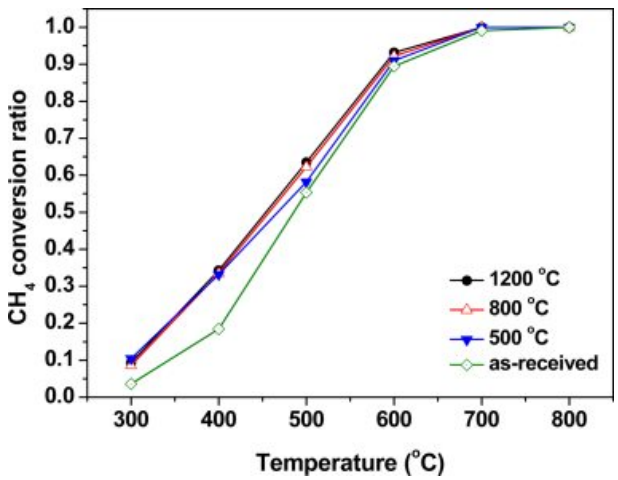

Fig. 4. SMR performance of the Ni/Al_2O_3 composites prepared by the hydrothermal-infiltration method according to heat-treatment temperatures of the Al_2O_3 support.

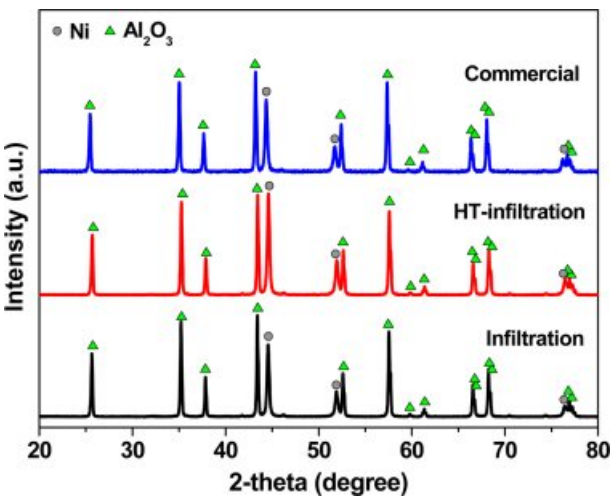

Fig. 6. XRD patterns of the Ni/Al_2O_3 composite according to the preparation technique.

Table 2. Elemental analysis based on the HR-SEM/EDS data at the surface and interior of the Ni/Al_2O_3 composite.

Sample	Surface (wt%)				Interior (wt%)			
	Ni	Al	O	Ni content in Ni/Al_2O_3	Ni	Al	O	Ni content in Ni/Al_2O_3
Infiltrated	39.00	34.19	26.81	37.65	12.96	48.01	39.03	12.50
Hydro-thermal	14.40	49.09	36.51	13.44	13.72	46.22	40.06	13.58

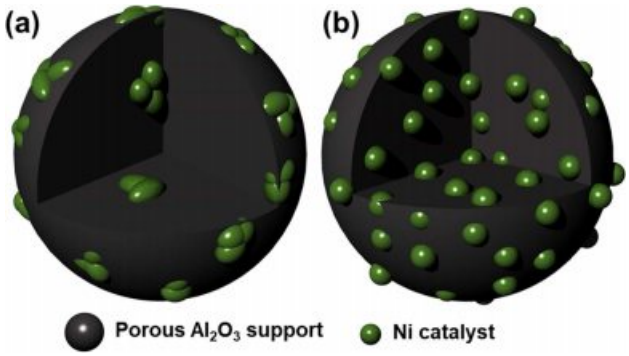

Fig. 7. Schematic illustration of the Ni/Al_2O_3 composite prepared by (a) the conventional infiltration method and (b) the hydrothermal-infiltration method.

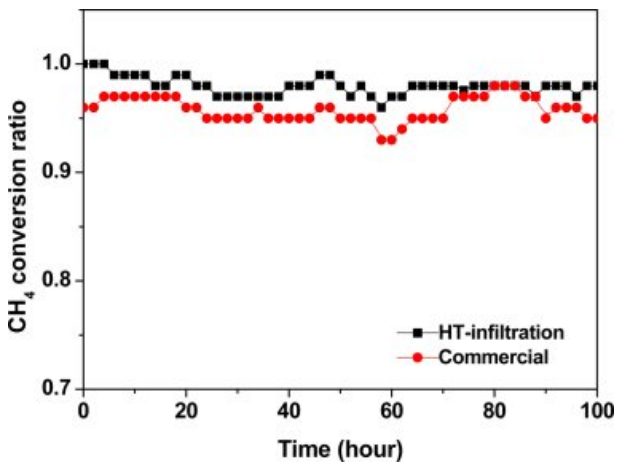

Fig. 8. Long-term stability of the Ni/Al_2O_3 composite prepared by the hydrothermal-infiltration method compared with the commercial catalyst at 600 ºC for 100 h.

composites prepared by the conventional infiltration method and hydrothermal-infiltration method is shown in Fig. 7. In the case of the sample prepared by the hydrothermal-infiltration method, the Ni catalyst is evenly distributed on the surface and inside the porous support, whereas in the case of the sample produced by the conventional impregnation method, the Ni catalyst is mainly aggregated and distributed on the surface of the support. Since the methane conversion reaction is proportional to the number of reaction sites, the sample produced by the hydrothermal-infiltration method with Ni catalysts evenly distributed inside and outside the support exhibited better SMR performance, as shown in Fig. 5.

Meanwhile, Fig. 8 shows the long-term stability of the Ni/Al_2O_3 composite prepared by the hydrothermal-infiltration method compared with the commercial catalyst at 600 ºC for 100 h. The Ni/Al_2O_3 composite prepared by the hydrothermal-infiltration method showed a higher methane conversion ratio at 600 ºC than the commercial catalyst. Moreover, no degradation in the SMR performance of the Ni/Al_2O_3 composite prepared by the hydrothermal-infiltration method was observed for 100 h.

Conclusions

Ni/Al_2O_3 composites as SMR catalysts were prepared successfully using the hydrothermal-infiltration method in this study. The heat-treatment temperature strongly affected the microstructure of the Al_2O_3 support. Significant grain growth and large interfacial necking occurred at 1,200 ºC, resulting in an increase in porosity and pore diameter. Therefore, the Ni/Al_2O_3 composite with the support fired at 1,200 ºC exhibited the best SMR performance due to a relatively large amount of Ni catalyst loading and easy diffusion of the reaction gas through the large pores. Moreover, the Ni/Al_2O_3 composite prepared by the hydrothermal-infiltration method showed much better SMR performance than that prepared by the conventional infiltration method because Ni catalysts could be distributed evenly throughout the porous support by the driving force of high temperature and high pressure during the hydrothermal-infiltration process. Meanwhile, the Ni/Al_2O_3 composite prepared by the hydrothermal-infiltration method showed a higher methane conversion ratio at 600 ºC than the commercial catalyst and no SMR performance degradation for 100 h. In this regard, the Ni/Al_2O_3 composite prepared by the hydrothermal-infiltration method can be a promising SMR catalyst due to its high performance and stability.

Acknowledgements

This work was supported by the National Research Foundation of Korea (NRF) grant funded by the Korea government (MSIT) (No. 2018R1A4A1025528). This work was also supported by the Technology Development Program to Solve Climate Changes of the National Research Foundation (NRF) grant funded by the Korea government (Ministry of Science and ICT) (2017M1A 2A2044930).

References

1. K. Tomishige, J. Jpn. Pet. Inst. 50 (2007) 287-298.
2. D.L. Li, Y. Nakagawa, and K. Tomishige, Appl. Catal. A408 (2011) 1-24.
3. H.S. Roh, Y. Jung, K.Y. Koo, U.H. Jung, Y.S. Seo, and W.L. Yoon, Chem. Lett. 38 (2009) 1162-1163.
4. C. Rameshan, W. Stadlmayr, C. Weilach, S. Penner, H. Lorenz, M. Havecker, R. Blume, T. Rocha, D. Teschner, and A. Knop-Gericke, Angew. Chem. Int. Ed. 49 (2010) 3224-3227.
5. M.A. Pená, J.P. Gómez, and J.L.G. Fierro, Appl. Catal. A 144 (1996) 7-57.
6. L.C. Silva, V.V. Murata, C.E. Hori, and A.J. Assis, Optim. Eng. 11 (2010) 441-458.
7. R. Faure, F. Rossignol, T. Chartier, C. Bonhomme, A. Maître, G. Etchegoyen, P. Del Gallo, and D. Gary, J. Eur. Ceram. Soc. 31 (2011) 303-312.
8. D.C. Grenoble, M.M. Estadt, and D.F. Ollis. J. Catal. 67 (1981) 90-102.
9. E. Chenu, G. Jacobs, and A.C. Crawford, Appl. Catal. B: Environmental, 59 (2005) 45-56.
10. F. Arena, A. Licciardello, and A. Parmaliana, Catal. Lett. 6 (1990) 139-149.
11. S.C. Dantas, J.C. Escritori, R.R. Soares, and C.E. Hori, Chem. Eng. J. 156 (2010) 380-387.
12. H.S. Roh, I.H. Eum, and D.W. Jeong, Renew. Energy 42 (2012) 212-216.
13. J.R. Rostrup-Nielsen and J.H.B. Hansen, J. Catal. 144 (1993) 38-49.
14. Y. Sakai, H. Saito, T. Sodesawa, and F. Nozaki, React. Kinet. Catal. Lett. 24 (1984) 253-257.
15. S.M. Baek, J.H. Kang, K. Lee, and J.H. Nam, Int. J. Hydrogen Energy 39 (2014) 9180-9192.
16. L. Roses, F. Gallucci, G. Manzolini, and M. van S. Annaland, Chem. Eng. J. 222 (2013) 307-320.
17. L.A. Rudnitskii, T.N. Solboleva, and A.M. Alekseev, React. Kinet. Catal. Lett. 26 (1984) 149-151.
18. N.C. Fan, Y.Y. Chen, K.Y. Chen, W.C.J. Wei, B.H. Liu, A.B. Wang, and R.C. Luo, J. Ceram. Proc. Res. 18(9) (2017) 676-682.
19. O. Tokunaga and S. Ogasawara, React. Kinet. Catal. Lett. 39 (1989) 69-74.
20. D.L. Li, Y. Nakagawa, and K. Tomishige, Appl. Catal. A 408 (2011) 1-24.
21. W. Wang, S.P. Jiang, I.Y. Toka, and L. Luo, J. Power Sources 159 (2006) 68-72.
22. S.P. Jiang, W. Wang, and J. Electrochem, Soc. 152 (2005) A1398-A1408.
23. S.P. Jiang, Mater. Sci. Eng. A 418 (2006) 199-210.
24. T. Adschiri, Y. Hakuta, and K. Arai, Ind. Eng. Chem. Res. 39 (2000) 4901-4907.
25. J. Yun, J.W. Lee, R.H. Song, and W. Tai, ECS Trans., 57 (2013) 2313-2319.
26. M. Yoshimura, S.T. Song, and S. Somiya, J. Ceram. Assoc. 90 (1982) 91-95.
27. J. Ortiz-Landeros, C. Gómez-Yáñez, R. López-Juárez, I. Dávalos-Velasco, and H. Pfeiffer, J. Adv. Ceram. 1 (2012) 204-220.
28. S.H. Cho, N.H. Hao, and T. Yamaguchi, J. Ceram. Proc. Res. 17[1] (2016) 41-45.